Arginine 107 of yeast ATP synthase subunit g mediates sensitivity of the mitochondrial permeability transition to phenylglyoxal

Guo, Lishu

2018-09-21

Guo , L , Carraro , M , Sartori , G , Minervini , G , Eriksson , O , Petronilli , V & Bernardi , P 2018 , ' Arginine 107 of yeast ATP synthase subunit g mediates sensitivity of the mitochondrial permeability transition to phenylglyoxal ' , Journal of Biological Chemistry , vol. 293 , no. 38 , pp. 14632-14645 . https://doi.org/10.1074/jbc.RA118.004495

http://hdl.handle.net/10138/252431
https://doi.org/10.1074/jbc.RA118.004495

publishedVersion

Arginine 107 of yeast ATP synthase subunit g mediates sensitivity of the mitochondrial permeability transition to phenylglyoxal

Received for publication, June 16, 2018, and in revised form, July 27, 2018 Published, Papers in Press, August 9, 2018, DOI 10.1074/jbc.RA118.004495

Lishu Guo[‡1], **Michela Carraro**[‡], **Geppo Sartori**[‡], **Giovanni Minervini**[‡], **Ove Eriksson**[§], **Valeria Petronilli**[‡], and **Paolo Bernardi**[‡2]

From the [‡]*Consiglio Nazionale delle Ricerche Institute of Neuroscience and Department of Biomedical Sciences, University of Padova, Padova 35131, Italy and the* [§]*Department of Biochemistry and Developmental Biology, Faculty of Medicine, University of Helsinki, Helsinki 00290, Finland*

Edited by John M. Denu

Modification with arginine-specific glyoxals modulates the permeability transition (PT) of rat liver mitochondria, with inhibitory or inducing effects that depend on the net charge of the adduct(s). Here, we show that phenylglyoxal (PGO) affects the PT in a species-specific manner (inhibition in mouse and yeast, induction in human and *Drosophila* mitochondria). Following the hypotheses (i) that the effects are mediated by conserved arginine(s) and (ii) that the PT is mediated by the F-ATP synthase, we have narrowed the search to 60 arginines. Most of these residues are located in subunits α, β, γ, ϵ, a, and c and were excluded because PGO modification did not significantly affect enzyme catalysis. On the other hand, yeast mitochondria lacking subunit g or bearing a subunit g R107A mutation were totally resistant to PT inhibition by PGO. Thus, the effect of PGO on the PT is specifically mediated by Arg-107, the only subunit g arginine that has been conserved across species. These findings are evidence that the PT is mediated by F-ATP synthase.

The mitochondrial PT[3] is a Ca^{2+}-dependent permeability increase of the inner membrane (1). The PT is mediated by opening of a regulated channel, the permeability transition pore (PTP), which coincides with the mitochondrial megachannel (MMC) identified by electrophysiology (2, 3). The mammalian PTP/MMC displays a range of conductance states, which can be as high as 1.2 nanosiemens, corresponding to a pore with a diameter of about 2 nm. The channel also visits lower conductance states that may be the basis for selective permeation of small solutes (4). Depending on open time and channel size, the PTP/MMC can participate in Ca^{2+} homeostasis (short-term and/or low-conductance openings that provide a pathway for fast Ca^{2+} release) (5) or cell death (long-lasting and/or high-conductance openings that cause energy dissipation, membrane permeabilization to solutes, matrix swelling, and outer membrane rupture with release of proapoptotic proteins) (6). The mammalian PTP is modulated by binding of cyclophilin D (CyPD), which favors pore opening after matrix accumulation of Ca^{2+}, an essential permissive factor (7). Regulation of the PTP is complex; opening is favored by CyPD, P_i, and oxidative stress, whereas it is inhibited by matrix H^+, Mg^{2+}, adenine nucleotides, and cyclosporin A, which displaces CyPD and desensitizes the pore to Ca^{2+} (8). Although the molecular components of the PTP were unknown, a few discrete regulatory sites have been defined in the 1990s through the use of modifiers of SH groups and of relatively specific histidine and arginine reagents (9–15).

The most recent hypothesis about the molecular nature of the PTP/MMC is that it originates from a conformational change occurring on F-ATP synthase when Mg^{2+} is replaced by Ca^{2+} at the catalytic site. The conformational change would be transmitted to the inner membrane by the peripheral stalk, causing pore formation at the interface between enzyme monomers (7). Whether and how the F-ATP synthase can form channels is the matter of controversy. The hypothesis is supported by genetic manipulation of F-ATP synthase (16, 17); by electrophysiological measurements of the bovine, human, yeast, and *Drosophila* enzymes (17–20); and by site-directed mutagenesis of specific F-ATP synthase residues (21, 22), whereas it has been questioned by studies based on genetic ablation of subunits c, b, and OSCP (23, 24) (see Bernardi and Lippe (25) for a recent discussion that covers this controversy and offers an explanation for the apparent discrepancies).

The PTP response to Ca^{2+} is modulated by arginine residues, which upon modification with glyoxals can cause PTP sensitization or desensitization, depending on the specific reagent (12–15). Previous studies have focused on the structure–function relationship of glyoxals of different structure rather than on the identification of the reactive residue(s) (12–15). Here, we have found that the effect of phenylglyoxal (PGO) on the PTP differs between species and used sequence comparison

This work was supported by AIRC Grant IG17067 (to P. B.) and Fondation Leducq Grant 16CVD04 (to P. B.). The authors declare that they have no conflicts of interest with the contents of this article.

[1] Supported by a fellowship from the China Scholarship Council. This work is in partial fulfillment of the requirements for the Ph.D. for this author at the Department of Biomedical Sciences, University of Padova.

[2] To whom correspondence should be addressed. Tel.: 39-049-827-6365; Fax: 39-049-827-6049; E-mail: bernardi@bio.unipd.it.

[3] The abbreviations used are: PT, mitochondrial permeability transition; AGE, advanced glycation end-products; CRC, Ca^{2+} retention capacity; CyPD, cyclophilin D; MGO, methylglyoxal; MLM, mouse liver mitochondria; MMC, mitochondrial megachannel; PGO, phenylglyoxal; PTP, permeability transition pore; YM, yeast mitochondria; MGO, methylglyoxal; BisTris, 2-[bis(2-hydroxyethyl)amino]-2-(hydroxymethyl)propane-1,3-diol; ANOVA, analysis of variance.

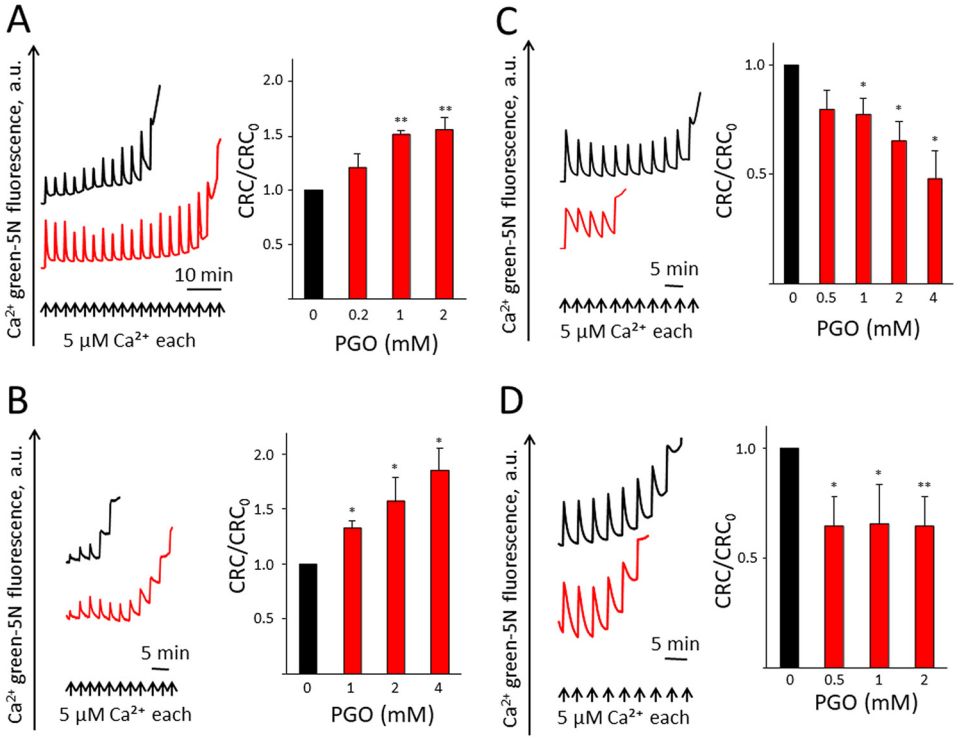

Figure 1. The sensitivity of PTP to PGO is conserved across species. Isolated mitochondria or permeabilized cells were pretreated with vehicle (DMSO) or PGO and resuspended in the CRC assay buffer as described under "Experimental Procedures." *A*, CRC of MLM pretreated with DMSO (*black trace*) or 1 mM PGO (*red trace*). *B*, CRC of isolated yeast mitochondria pretreated with DMSO (*black trace*) or 4 mM PGO (*red trace*). *C*, CRC of permeabilized HEK293 cells pretreated with DMSO (*black trace*) or 4 mM PGO (*red trace*). *D*, CRC of permeabilized *Drosophila* S_2R^+ cells pretreated with DMSO (*black trace*) or 1 mM PGO (*red trace*). Representative traces are shown. *Bars*, CRC of DMSO- (*black*) or PGO-pretreated (*red*) isolated mitochondria or permeabilized cells. CRC of DMSO-treated mitochondria was set as 1 unit. Results are mean ± S.E. (*error bars*) of at least three independent experiments. *, $p < 0.05$ *versus* vehicle; **, $p < 0.01$ *versus* vehicle. One-way ANOVA was used for statistical analysis.

and mutagenesis to identify the unique arginine of F-ATP synthase subunit g (of a total of 60 conserved residues) that mediates the PTP-modulating effect of PGO in yeast. This finding is a step forward in the molecular understanding of PTP regulation and further supports the hypothesis that the PTP forms from F-ATP synthase.

Results

The effects of PGO on the PTP have been conserved but differ between species

Consistent with the effect of PGO on the PTP of rat liver mitochondria, PGO desensitized the PTP to Ca^{2+} in mouse liver mitochondria (MLM) (Fig. 1*A*) as well as in mitochondria from *Saccharomyces cerevisiae* in the presence of ETH129, a selective ionophore that allows Ca^{2+} equilibration across the inner membrane in yeast mitochondria (Fig. 1*B*). In either case, the desensitizing effect can be appreciated from the increased Ca^{2+} retention capacity (CRC) of PGO-treated mitochondria (Fig. 1, *A* and *B*). Unexpectedly, PGO caused instead sensitization of the pore to Ca^{2+} in permeabilized human HEK293 (Fig. 1*C*) and *Drosophila* S_2R^+ cells (Fig. 1*D*). Sensitization of PTP opening by PGO in human and *Drosophila* cells was not due to digitonin permeabilization, as it was also observed in mitochondria isolated from these cells (results not shown). These findings indicate that the ability to modulate the PTP by PGO has been conserved across species. Under the assumptions (i) that the observed differences depend on specific features of the PTP rather than on the existence of species-specific reactive sites and (ii) that these sites are located on the F-ATP synthase, we narrowed the search of the reactive arginine(s) from 135 (yeast) to 60 arginines that are conserved between F-ATP synthases of *S. cerevisiae*, *Homo sapiens*, *Mus musculus*, and *Drosophila melanogaster* (the positions of these residues in the yeast, human, and mouse enzymes are reported in Table 1).

Chemical modification by PGO does not affect catalytic activity, oligomycin sensitivity, assembly, and subunit composition of F-ATP synthase

Due to the large number of arginine residues and their specific relevance to enzymatic activity of F-ATP synthase, we assessed whether treatment with PGO affects the catalytic properties of the enzyme in MLM and yeast mitochondria (YM). In MLM, a trend toward a slight inhibition of ATP hydrolysis was observed (but this did not reach statistical significance), and the catalytic activity maintained its sensitivity to oligomycin (Fig. 2*A*), and respiratory stimulation by ADP was not affected (Fig. 2*B*). Similarly, in YM, both ATP hydrolytic activity and respiratory stimulation by ADP were unaffected by PGO (Fig. 2, *C* and *D*). Blue native gel separation and in-gel activity staining after digitonin extraction did not reveal any major effect of PGO on F-ATP synthase oligomeric state in MLM (Fig. 2*E*). In these experiments, we used MLM because they are easy to purify and because the mouse enzyme is virtu-

Table 1
Number and positions of arginine residues conserved between F-ATP synthase of *S. cerevisiae*, *H. sapiens*, and *M. musculus* (in parentheses when different)

Subunit	Total number	Positions in *S. cerevisiae*	Positions in *H. sapiens* (*M. musculus*)
α	26	4, 9, 67, 77, 127, 143, 163, 165, 176, 198, 201, 208, 225, 247, 295, 316, 323, 324, 328, 341, 345, 399, 410, 435, 457, 460	5, 12, 73, 83, 133, 149, 169, 171, 182, 204, 207, 214, 231, 253, 301, 322, 329, 330, 334, 347, 351, 405, 416, 441, 463, 466
β	17	93, 105, 127, 139, 223, 225, 262, 264, 277, 293, 307, 328, 370, 389, 439, 441, 445	109, 121, 143, 155, 239, 241, 279, 281, 294, 310, 324, 345, 387, 406, 456, 458, 462
γ	7	4, 31, 42, 153, 266, 290, 292	4, 23, 34, 143, 253, 277, 279
a	1	186	159
c	1	39	c1: 99, c2: 104 (109), c3: 105 (104)
ϵ	2	5, 23	6, 24
OSCP	2	8, 114	14, 117
b	1	200	208
f	1	56	50 (44)
e	1	8	15
g	1	107	96
Total	60	60	60

ally identical to the human and yeast species for composition of conserved arginines (Table 1). Analysis of dimers and monomers resolved by SDS-PAGE and silver staining demonstrated that treatment with PGO did not alter the pattern and relative abundance of F-ATP synthase subunits (Fig. 2*F*). Based on these results, the arginine residues of the F_1 sector, subunit a, and c-ring were not investigated further. Taking advantage of the yeast model and of the species-specific response to PGO, we performed a set of mutagenesis experiments in yeast cells to identify the arginine residue(s) conferring the modulatory effect to PGO.

OSCP does not confer sensitivity to the effects of PGO

We first investigated whether OSCP, which contains two conserved arginine residues (Table 1), could be involved in conferring the species specificity to the effects of PGO, which are opposite in human and yeast mitochondria (Fig. 1). Deletion of the *ATP5* gene encoding for OSCP (Δ*ATP5*) prevented F-ATP synthase assembly and growth on glycerol, both features being rescued by reexpression of the WT yeast gene (Δ*ATP5* + yOSCP) (Fig. 3, *A–C*). Replacement with the human OSCP gene (Δ*ATP5* + hOSCP) was instead essentially unable to rescue F-ATP synthase assembly unless the yeast mitochondrial targeting sequence replaced the human sequence in the construct (Δ*ATP5* + yhOSCP). Indeed, only the chimeric protein allowed assembly of a functional F-ATP synthase complex, which grew normally on glycerol (Fig. 3, *A–C*). The rescued mutant displayed an increased CRC in response to PGO (*i.e.* the same response of WT yeast mitochondria) (Fig. 3*D*). Thus, OSCP does not confer species specificity to the effects of PGO on the PTP.

Arginine 107 of yeast F-ATP synthase subunit g mediates the effect of PGO on the mitochondrial permeability transition

Both subunit e and g possess a conserved arginine residue (Arg-8 and Arg-107 in the yeast sequence, respectively, Fig. 4). These residues correspond to Arg-15 and Arg-96, respectively, in the human sequence (Table 1). To test whether these residues are involved in PTP modulation by PGO, we first analyzed deletion mutants of subunit g (Δ*ATP20*) and of subunit e (Δ*TIM11*). The effect of PGO was completely abolished in the Δ*ATP20* deletion mutant lacking subunit g (Fig. 5*A*), and a similar, albeit somewhat smaller, effect was observed with the Δ*TIM11* mutant lacking subunit e (Fig. 5*B*). To explore the role of individual arginines, we generated specific point mutants and tested their CRC. Remarkably, the R107A mutation in subunit g dramatically blunted the effect of PGO (Fig. 5*C*), whereas the R8A mutation in subunit e was ineffective, with an identical sensitivity to PGO as the WT species (Fig. 5*D*). This result was puzzling because subunit e only has one conserved arginine in position 8, and therefore we would have expected the same result following either deletion of the subunit e gene or the R8A mutation. This apparent contradiction was resolved by analysis of the expression of the e and g subunits in the Δ*ATP20* and Δ*TIM11* mutants. Indeed, deletion of the *ATP20* gene led to the expected disappearance of subunit g only, whereas deletion of the *TIM11* gene caused the disappearance of both subunit e and g (Fig. 5*E*). Both Arg-8 and Arg-107 are located next to the G*XXX*G dimerization domains (Figs. 4 and 5*F*), and we suspect that this is the region where the PTP forms.

The ATP20 Arg-107 mutation does not affect growth properties, dimerization, and subunit composition of F-ATP synthase

Given the importance of subunits e and g in both F-ATP synthase dimerization and PTP formation in yeast (19), we characterized the key features of the R107A mutants. Yeast cells can grow by fermentation in glucose-rich medium, whereas they need ATP generated from oxidative phosphorylation in glycerol medium. The ATP20 R107A mutant grew both on the glucose and glycerol (Fig. 6*A*), indicating that the mutation did not influence the function of F-ATP synthase. The Δ*TIM11* and Δ*ATP20* mutants expectedly did not display dimers after digitonin extraction and blue native PAGE (Fig. 6*B*). Mitochondria

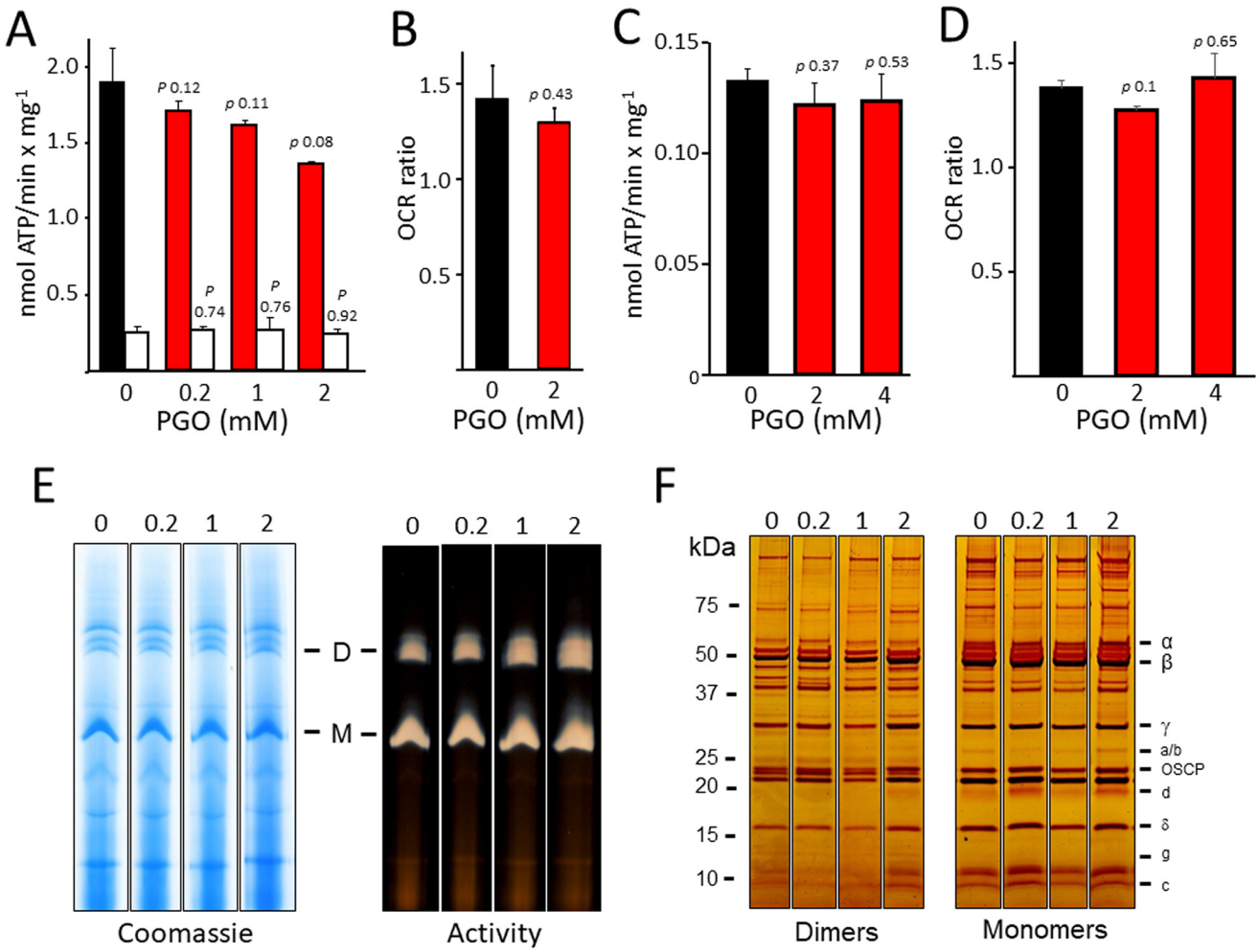

Figure 2. Chemical modification of arginine residue(s) by PGO does not significantly affect activity, dimerization, and assembly of F-ATP synthase. Experimental conditions were as described under "Experimental procedures." *A*, ATP hydrolysis rate of MLM pretreated with DMSO (*black bar*) or with the indicated concentrations of PGO (*red bars*). *Closed bars*, values subtracted for the oligomycin-insensitive fraction and expressed as nmol of ATP/mg/min. *Open bars*, ATP hydrolysis in the presence of 4 μM oligomycin. Results are mean ± S.E. (*error bars*) of three independent experiments. *B*, oxygen consumption rate of DMSO- or 2 mM PGO-pretreated MLM in presence of succinate (state 4) and ADP + P_i (state 3). Values refer to state 3/state 4 ratio and are expressed as mean ± S.E. of three independent experiments. *C*, ATP hydrolysis rate of YM isolated from WT strain BY4743 pretreated with DMSO (*black bar*) or with the indicated concentrations of PGO (*red bars*). Values have been subtracted for the oligomycin-insensitive fraction and expressed as nmol of ATP/mg/min. Results are mean ± S.E. of at least three independent experiments. *D*, oxygen consumption rate of YM isolated from WT strain BY4743 pretreated with DMSO (*black bar*) or with the indicated concentrations of PGO (*red bars*) in the presence of NADH and ADP. Values refer to the ratio of OCR (ADP) and OCR (NADH) and are expressed as mean ± S.E. of three independent experiments. *E*, isolated MLM pretreated with the concentrations of PGO labeling each lane were separated by BN-PAGE as described under "Experimental procedures" and revealed with Coomassie Blue and in-gel activity staining for ATP hydrolysis to identify dimers (*D*), monomers (*M*), and F_1 sector of F-ATP synthase. *F*, dimers and monomers were cut out from BN-PAGE gels and subjected to SDS-PAGE and silver-stained. All sets of lanes in *E* and *F* are from the same gels.

reexpressing either WT or R107A subunit g had functional dimers indistinguishable from those of WT BY4743 cells (Fig. 6*B*) with identical subunit composition, as judged from SDS-PAGE and silver staining (Fig. 6*C*). Thus, the R107A replacement in subunit g did not influence the assembly, activity, and stability of F-ATP synthase.

PGO reacts with Arg-107 of subunit g and affects the pore only in mitochondria with the WT subunit

We next tested whether the PGO adduct affects the properties of the PTP. One emerging issue is pore size, which is affected by the deletion of lateral stalk subunits OSCP and b even when the CRC is apparently unaffected (24). We therefore measured Ca^{2+}-induced swelling in yeast mitochondria in the presence of ETH129 to allow electrophoretic Ca^{2+} uptake. The swelling rate was significantly inhibited by PGO in mitochondria reexpressing WT subunit g but not the R107A mutant, which displayed a lower rate of swelling (Fig. 7, *A–C*). Because yeast subunit g also contains an arginine residue at position 106, we employed synthetic test peptides corresponding to the 88–114 amino acid segment of WT or containing the R106A replacement. Following reaction with PGO, the peptides were analyzed by MALDI-TOF MS. The results revealed that one adduct with a molecular mass of 116 Da was formed on both the WT and the R106A modified peptide (Fig. 7*D*). This molecular mass corresponds to one molecule of PGO covalently attached to the guanidine moiety of arginine. Formation of one single adduct in the WT peptide carrying two adjacent arginines suggests that reaction of Arg-107 with PGO may reduce the reactivity of Arg-106.

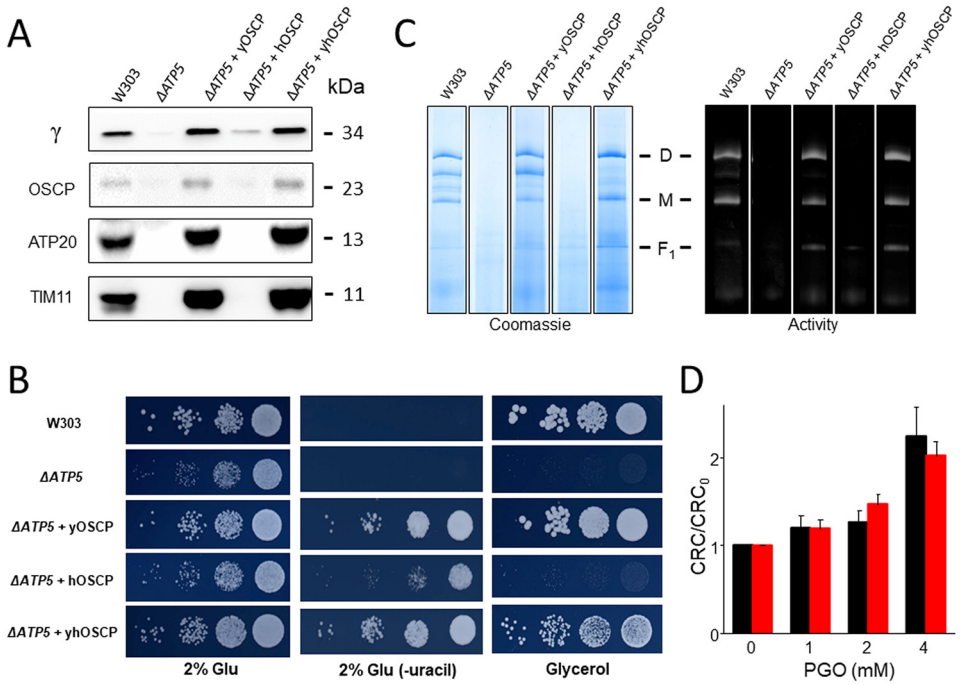

Figure 3. Expression of human OSCP does not alter the inhibitory effect of PGO on yeast PTP. *A*, isolated yeast mitochondria of the indicated genotypes (50 μg of protein/lane) were evaluated by Western blotting for γ, OSCP, *TIM11*, and *ATP20* subunits. *B*, serial dilution spotting assay of the indicated genotypes. Cell suspensions were grown to $A_{600\ nm} = 1$; serially diluted; plated on medium containing 2% glucose (*Glu*), 2% Glu drop-out uracil (−*uracil*), and 2% glycerol; and incubated at 30 °C. Pictures were taken after 1–2 days. *C*, yeast mitochondrial proteins of the indicated genotypes were separated by BN-PAGE as described under "Experimental procedures," and revealed with Coomassie Blue and in-gel activity staining for ATP hydrolysis to identify dimers (*D*), monomers (*M*), and F_1 sector of F-ATP synthase. *D*, CRC of yeast mitochondria from Δ*ATP5* + yOSCP (*black bars*) and Δ*ATP5* + yhOSCP (*red bars*) pretreated with the indicated concentrations of PGO. Data are expressed as CRC/CRC_0 ratio, in which CRC_0 refers to the CRC of DMSO-treated mitochondria. Results are mean ± S.E. (*error bars*) of at least three independent experiments. All sets of lanes in *A* and *C* are from the same gels.

Expression of human subunit g in yeast prevents PGO-dependent desensitization of PTP

PGO desensitizes the yeast PTP to Ca^{2+} (thus increasing the CRC), whereas it sensitizes it in human HEK293 cells (thus decreasing the CRC; see Fig. 1). We exploited this phenotypic difference to test whether expression of human subunit g is able to switch the inhibitory effect of PGO in yeast mitochondria to the inducing effect seen in human mitochondria. Deletion of the *ATP20* gene encoding for yeast subunit g prevented dimerization of F-ATP synthase, which could be rescued by both expression of *ATP20* and of *ATP5L* (which encodes human subunit g) (Fig. 8*A*). As for WT yeast (compare with Fig. 1), PGO increased the CRC of Δ*ATP20* mitochondria reexpressing *ATP20*, whereas replacement with *ATP5L* totally prevented the desensitizing effects of PGO, which rather decreased the CRC (Fig. 8*B*), as also seen in permeabilized HEK293 cells. These results suggest that subunit g confers species specificity to the effects of PGO on the PTP.

Arg-107 of subunit g is a target for modification by high glucose, phenylglyoxal, and methylglyoxal

Advanced glycation end-products (AGE) originate from nonenzymatic modification of lysine and arginine residues that takes place after long-term exposure to high concentrations of glucose or to reactive compounds like methylglyoxal (MGO), a byproduct of glycolysis that alters protein structure, stability, and function (26–28). Yeast cells grown at high glucose concentration undergo protein glycation largely due to generation of high levels of MGO (29), with a relevant increase in argpyrimidine-modified proteins (30, 31). Arginine residues are frequently found in enzyme sites involved in substrate binding and catalysis, and their modification by MGO results in the formation of AGE (28). Consistent with these toxic effects, the growth rate of yeast cells was slowed down in high-glucose medium (Fig. 9*A*). At normal concentrations of glucose, toxicity was mimicked by PGO and MGO (Fig. 9*A*). Remarkably, yeast strains lacking subunit g or harboring the subunit g R107A mutation were significantly more resistant to PGO toxicity (Fig. 9*B*).

Discussion

The molecular nature of the PTP is a long-standing mystery of mitochondrial biology. In the past, we have used relatively selective sulfhydryl, histidine, and arginine reagents to define the properties of discrete sites conferring PTP regulation by the proton electrochemical gradient, divalent cations, quinones, and oxidative stress (8). The recent hypothesis that the PTP may originate from a specific, Ca^{2+}-induced conformation of F-ATP synthase (16–19) provides a unique opportunity to identify these sites in molecular terms. Indeed, mutagenesis of specific residues or deletion of specific subunits of F-ATP synthase should modify predictably the properties of the PTP and/or the effect of reagents acting at these sites. This is a formidable challenge because F-ATP synthase is a complex multisubunit enzyme (32–37) whose assembly is affected by deletion of specific subunits (23, 24). The present study is part of our

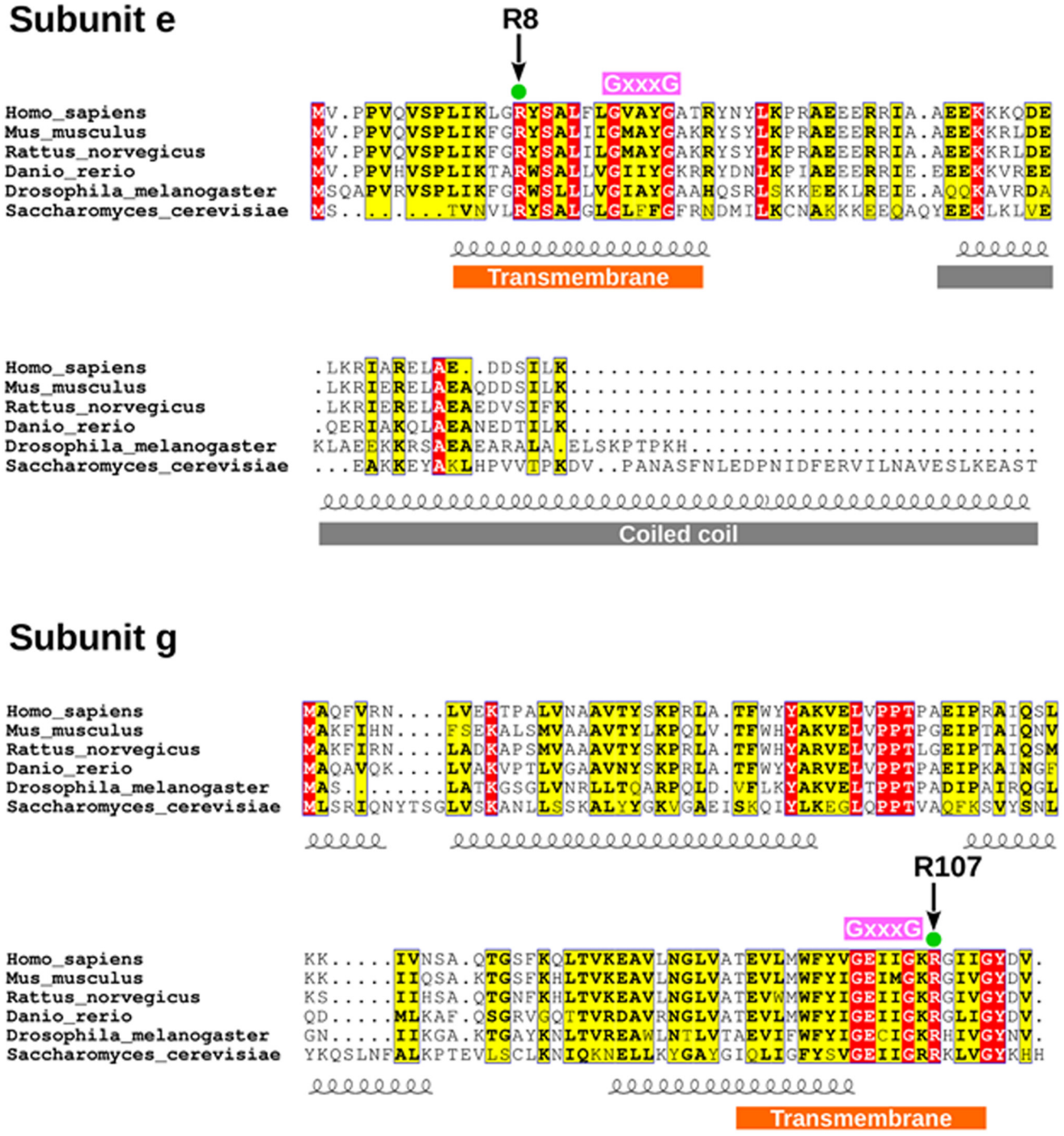

Figure 4. Amino acid sequence comparison of F-ATP synthase subunits e and g.

efforts at identifying such regulatory sites and, as a corollary, at (dis)proving the general hypothesis that the PTP originates from F-ATP synthase. So far, we have provided evidence (i) that Ca^{2+} triggers the PTP by substituting Mg^{2+} at the catalytic site, causing a conformational change that is transmitted through OSCP to the lateral stalk and eventually to the inner membrane (21), and (ii) that PTP blockade by matrix H^+ is mediated by the unique, highly conserved histidine residue of OSCP subunit (22). Here, we have been able to identify a unique arginine residue that mediates the effects of PGO on the Ca^{2+} sensitivity of the PTP in yeast mitochondria.

Our previous studies had defined the PTP-modulatory effects of arginine-selective reagents like glyoxals and 2,3-butanedione (12–15). Although glyoxals can also react with other residues (such as lysines and cysteines) (38), it has been possible to trace their effects on the PT to modification of arginines with reasonable certainty (12–15). In rat liver mitochondria, the outcome depended on the specific glyoxal used, with PTP inhibition by MGO or PGO and PTP activation by OH-PGO (12–15). Studies with a variety of compounds with similar reactivity but different overall physical-chemical properties led to the conclusion that glyoxals react with the same arginine residue(s) and

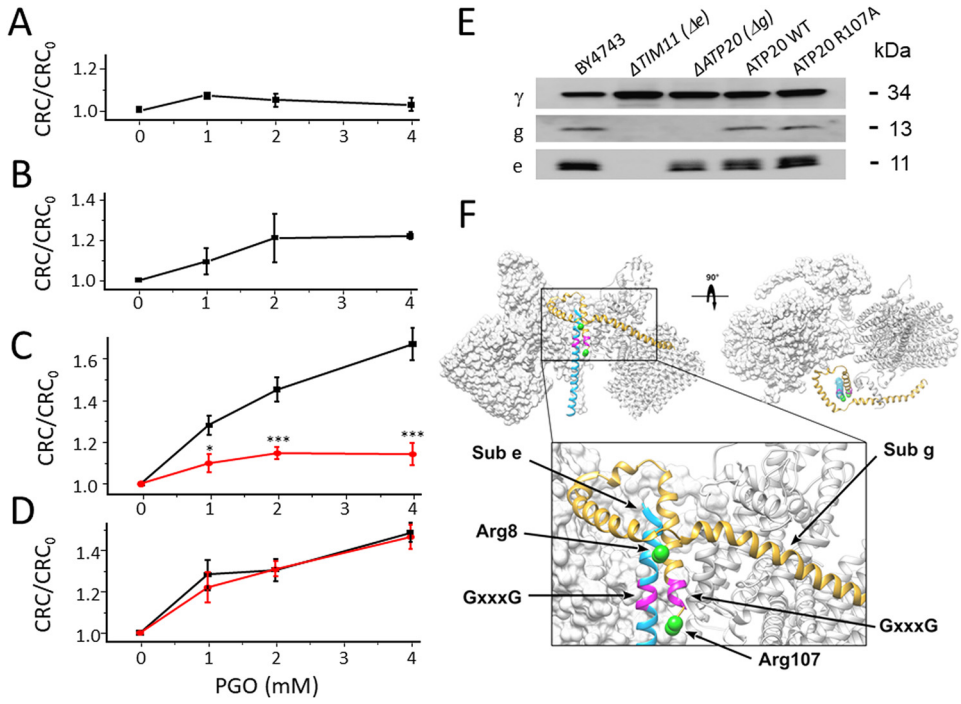

Figure 5. Arg-107 of yeast F-ATP synthase subunit g mediates the effects of PGO on the CRC. Experimental conditions were as in Fig. 1*B*. *A*, CRC of Δ*ATP20* yeast mitochondria pretreated with the indicated concentrations of PGO. *B*, CRC of Δ*TIM11* yeast mitochondria pretreated with the indicated concentrations of PGO. *C*, CRC of yeast mitochondria from ATP20 WT control (*black trace*) and ATP20 R107A (*red trace*) pretreated with the indicated concentrations of PGO. *, $p < 0.05$ *versus* ATP20 WT; ***, $p < 0.001$ *versus* ATP20 WT. Two-way ANOVA was used for statistical analysis. *D*, CRC of yeast mitochondria from TIM11 WT control (*black trace*) and TIM11 R8A (*red trace*) pretreated with the indicated concentrations of PGO. In *A–D*, data are expressed as ratio to DMSO-treated mitochondria. Means ± S.E. (*error bars*) of at least three independent experiments are shown. *E*, isolated yeast mitochondria of the indicated genotypes were evaluated by Western blotting for γ, *TIM11*, and *ATP20* subunit content after SDS-PAGE separation of 50 μg of protein per lane. *F*, overview of ATP synthase F_0 dimer (Protein Data Bank code 6B2Z) with *frontal* and *top views* highlighting the relative position of subunits g (*yellow*) and e (*light blue*). Putative G*XXX*G dimerization motifs are represented in *purple*. The structure is shown in standard view (*front*) and after a 90° rotation around the *z* axis, and two F_0 monomers are presented. The *boxed region* is expanded in the *bottom part* of the *panel*. *Green spheres* represent the position of Arg-8 of subunit e and Arg-107 of subunit g, which are predicted to localize at the border of the G*XXX*G domains. These positions were derived by comparing data from the three-dimensional structure (Protein Data Bank code 6B2Z) with secondary structure predictions.

that the main determinants for the effects on the PTP are charge and hydrogen-bonding capacity of the adducts (12–15). Here, we have added the very relevant piece of information that PGO has species-specific effects on the PTP. Having identified Arg-107 of subunit g as the unique target of PGO in yeast, we suspect that the species-specific effects may depend on differences in the primary structure of F-ATP synthase, which appear to be particularly prominent in subunits e and g (Fig. 4).

A large fraction of the 60 conserved arginines of F-ATP synthase is located in the catalytic sector (26 in subunit α and 17 in subunit β) and in the F_0 subunits γ, ϵ, c, and a (11 residues). The membrane extrinsic region (F_1 sector) of the F-ATP synthase complex is composed of 3α and 3β and of one each of the γ, δ, and ϵ subunits. The 3α3β hexamer contains the catalytic sites responsible for ATP synthesis or hydrolysis (32) and associates through the γ, δ, and ϵ subunits with a ring of hydrophobic c subunits (the c-ring) in the membrane domain. The rotating c-ring is in contact with the static a subunit, which maintains a specific pathway for translocation of protons through the membrane (34). A conserved arginine residue of subunit a plays a critical role in blocking a futile proton shortcut and in facilitating proton transfer at the a/c-ring interface via a carboxylic group in the c-ring (39). Our data do not reveal whether the arginine residues of the catalytic sector react with glyoxals, but they do indicate that, if present, these adducts do not play a direct role in PTP modulation.

OSCP plays a critical role in the assembly and function of F-ATP synthase (40, 41) and has a well-characterized regulatory role in PTP modulation in mammals by providing a site for CyPD binding, which results in sensitization of the PTP to Ca^{2+} (17, 42, 43). Replacement of yeast with human OSCP did not reverse PTP sensitization to Ca^{2+} by PGO, however, suggesting that also OSCP arginines are not critical for PTP modulation by glyoxals.

F-ATP synthase complexes associate into dimers, which are essential for the formation of oligomers and generation of the cristae (44–46). Subunits e and g are essential for this process, and deletion of either subunit leads to dimer and cristae disruption (46–52). The e and g subunits are also important for regulation of the Ca^{2+} sensitivity of yeast PTP, which undergoes desensitization after their genetic ablation (19). The fact that their contribution has been so far addressed in null mutants inevitably limits our understanding of their putative function in PTP formation. Conversely, site-directed mutagenesis of specific residues that does not alter assembly, subunit composition, and enzymatic activity of the enzyme allows interrogation of their role in PTP formation and regulation.

The yeast R107A mutant of subunit g described here shows F-ATP synthase dimers with normal hydrolytic activity, yet it displays a PTP that is desensitized to Ca^{2+} (data not shown) and insensitive to PGO and a decreased swelling rate in sucrose. This last finding suggests that Arg-107 of subunit g may be

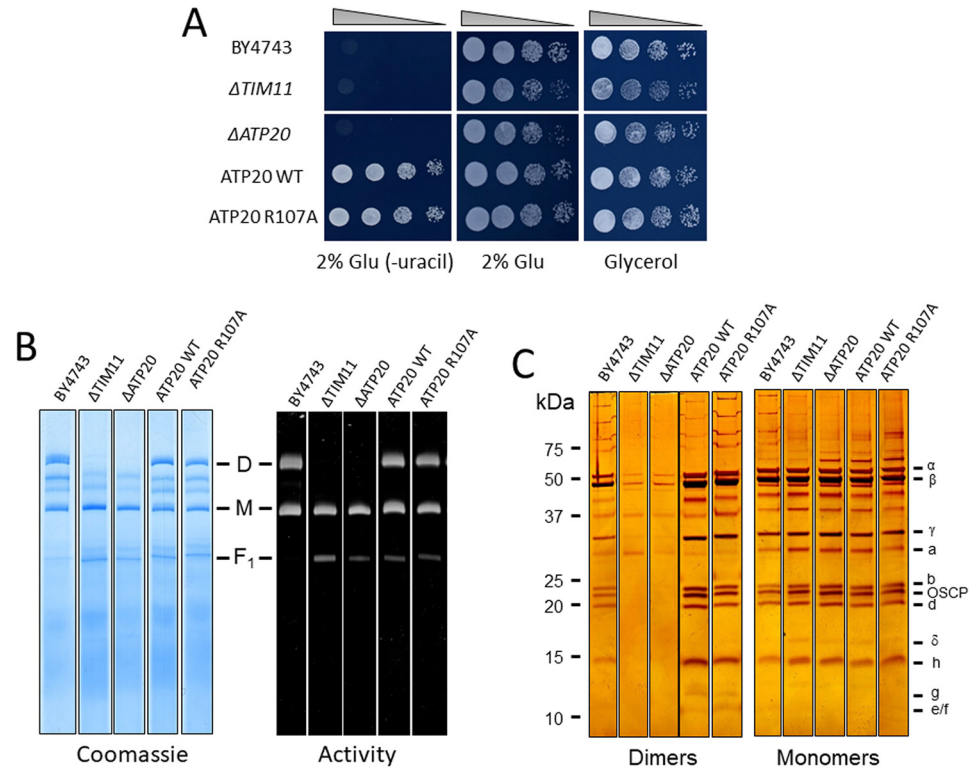

Figure 6. The ATP20 R107A mutation does not affect dimerization, assembly, and function of F-ATP synthase. *A*, serial dilution spotting assay of BY4743, Δ*TIM11*, Δ*ATP20*, ATP20 WT, ATP20 R107A strains. Cell suspensions were grown to $A_{600\,nm} = 1$; serially diluted; plated on medium containing 2% Glu, 2% Glu drop-out uracil (−*uracil*), and 2% glycerol; and incubated at 30 °C. Pictures were taken after 1–3 days. *B*, yeast mitochondrial proteins of the indicated genotypes were separated by BN-PAGE as described under "Experimental procedures" and revealed with Coomassie Blue and in-gel activity staining for ATP hydrolysis to identify dimers (*D*), monomers (*M*), and the F_1 sector of F-ATP synthase. *C*, dimers and monomers were cut out from BN-PAGE, subjected to two-dimensional SDS-PAGE, and revealed by silver staining. All sets of lanes in *B* and *C* are from the same gels.

important for solute permeation through the PTP, providing a further clue as to a possible site where the pore forms. Of note, replacement of yeast subunit g with its human counterpart confers the "human" phenotype to yeast, suggesting that the species-specific effect of PGO is more likely to depend on structural differences between the yeast and human F-ATP synthase than on the Arg-107–PGO adduct as such.

In mammals, dysregulated PTP opening is a primary cause of cell death initiated via matrix swelling and rupture of the outer membrane followed by release of proapoptotic factors (cytochrome *c*), whereas its inhibition appears often to be protective (8). Whether the pore plays a similar role in yeast is still a matter of debate. Yeast does not possess a mitochondrial Ca^{2+} uniporter to mediate rapid Ca^{2+} overload; nor does it form the apoptosome complex required for the activation of effector caspases. However, yeast mitochondria can undergo membrane permeabilization in response to Ca^{2+} and oxidative stress (53, 54), leading to the release of cytochrome *c*, which certainly causes decreased respiration and ATP production. These events, together with the activation of the yeast metacaspase Ycalp, are proximal events in yeast programmed cell death (54). Thus, as for mammals, PTP opening might represent an important cell death pathway also for yeast, which can undergo apoptosis and aging (55).

AGE arising from carbonyl stress contribute to many pathological states, such as diabetes and age-related diseases (26–28). It is apparent that adducts form at many sites other than subunit g, yet our findings suggest that altered PTP features may play a role in glucose-dependent toxicity also in human cells, as was already suggested (56). Whether additional arginine residues mediate the glyoxal-specific effects described in rat mitochondria and human cells (12–15) remains to be established. However, the demonstration that a single conserved arginine residue of subunit g mediates the effects of PGO on the PTP in yeast is another step toward a molecular understanding of PTP regulation and evidence that the latter forms from a specific conformation of the F-ATP synthase.

Experimental procedures

Reagents and cells

PGO hydrate, MGO, oligomycin, rotenone, succinic acid, pyruvate, alamethicin, ATP, ADP, EGTA, $CaCl_2$, digitonin, NADH, ETH129, galactose, and sucrose were from Sigma (Milan, Italy). Cyclosporin A was purchased from Calbiochem. Ca^{2+} Green-5N was from Invitrogen (Milan, Italy). HEK293T were obtained from the American Tissue Culture Collection (ATCC) and cultured in Dulbecco's modified Eagle's medium (Lonza, Basel, Switzerland) supplemented with fetal bovine serum (10%) and penicillin and streptomycin (1%) (Thermo Fisher Scientific). *Drosophila* Schneider S2 cells were obtained from Dr. Michael Forte (Oregon Health and Science University) and cultured as described (57). The *Saccharomyces cerevisiae* strains BY4743, Δ*TIM11*, and Δ*ATP20* were purchased from Thermo Scientific, and mitochondria were isolated as described (19). Antibodies for TIM11, ATP20, and γ subunits

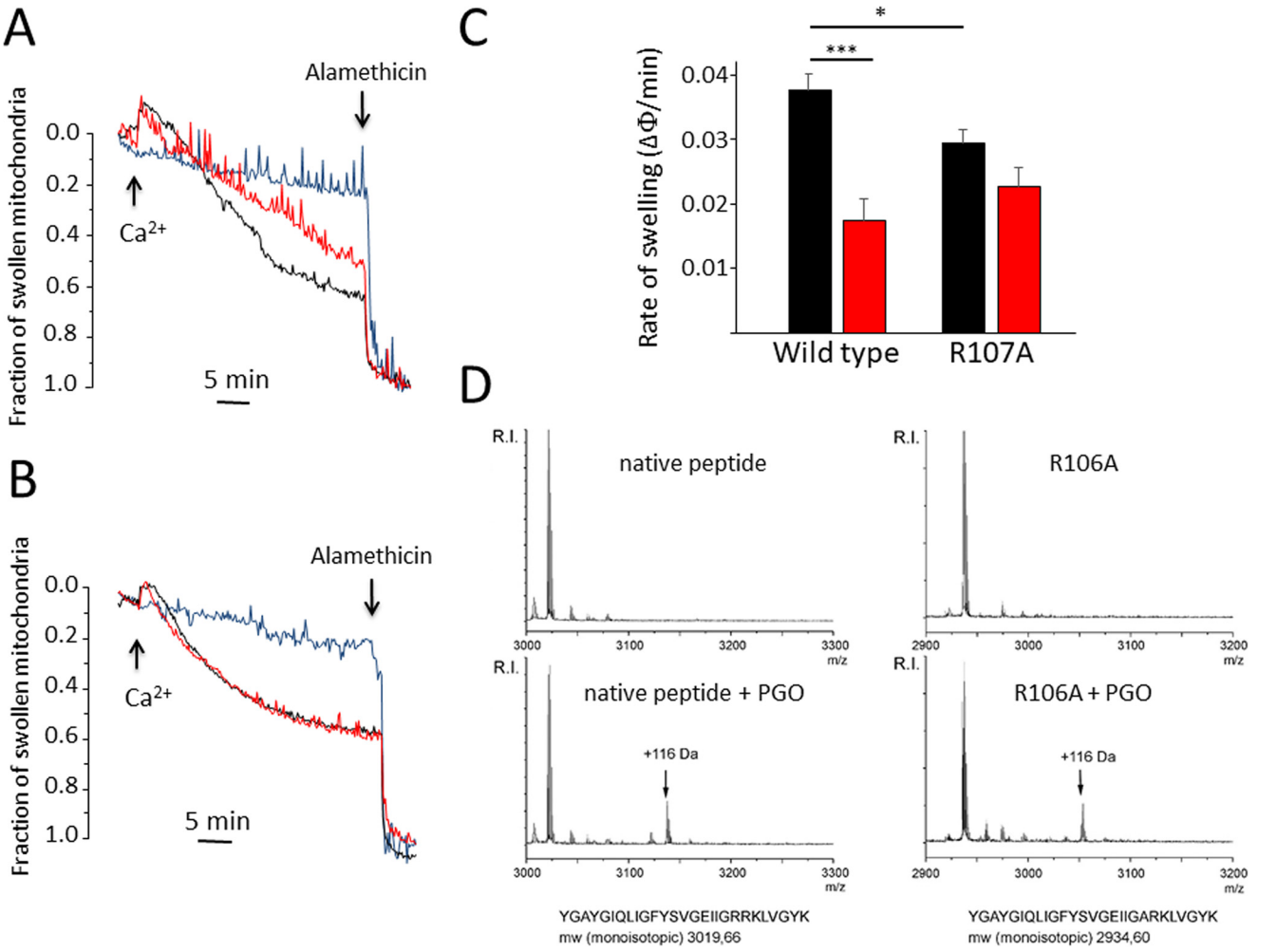

Figure 7. Arg-107 of yeast F-ATP synthase subunit g mediates inhibition of mitochondrial permeability transition by PGO. Experimental conditions were as in Fig. 1*B* except that Ca^{2+} green-5N was omitted. *A* and *B*, PTP-dependent mitochondrial swelling was evaluated as the decrease of absorbance at 540 nm, and the fraction of mitochondria that underwent the PT was assessed as described by Petronilli *et al.* (63). Additions of 50 μM Ca^{2+} and 5 μM alamethicin are indicated by *arrows*. Ca^{2+} was omitted in the *light blue traces*. Mitochondria isolated from ATP20 WT (*A*) and ATP20 R107A yeast (*B*) were treated with DMSO (*black traces*) or 4 mM PGO in DMSO (*red traces*). Representative traces of at least three independent experiments are shown. *C*, rate of mitochondrial swelling triggered by 50 μM Ca^{2+}. ATP20 WT or ATP20 R107A mitochondria were pretreated with DMSO (*black bars*) or 4 mM PGO (*red bars*). The rate of mitochondrial swelling is expressed as the fraction of swollen mitochondria/min. Data are mean ± S.E. (*error bars*) of at least three independent experiments. *, $p < 0.05$ *versus* WT (ATP20 WT); ***, $p < 0.001$ *versus* vehicle. One-way ANOVA was used for statistical analysis. *D*, MALDI-TOF mass spectra of synthetic peptides of the amino acid segment comprising Arg-107. The mass spectra of the parent peptides are shown in the *top windows*, and that of the PGO-modified peptides is shown in the *bottom window*. Masses in the spectra are $M + H^+$. The 116-Da adducts are marked with *arrows*.

were a kind gift of Dr. Marie-France Giraud (University of Bordeaux, France). Antibody for the OSCP subunit was purchased from Santa Cruz Biotechnology, Inc. (sc-365162).

Yeast mutant generation

To generate Δ*ATP5* yeast expressing the human or yeast OSCP (*ATP5*) sequence, the *ATP5* gene was first deleted in W303 diploids by substituting the genomic sequence with the Kan cassette of pFA6a-KanMX4 vector. Then diploids were allowed to sporulate in 2% potassium acetate medium, resulting tetrads were dissected, and correct clones were checked by semiquantitative PCR using appropriate primers. Yeast *ATP5* gene (yOSCP) was cloned in pFL38-URA vector after amplification using the following primers that include upstream and downstream regulatory sites (endogenous promoter and termination sequence): 5′-CACGACGTTGTAAAACGACGGCCAGTGAATTCGAGCTCGGTACCCTGCCGTCGTCATAAAGTGGAC (forward) and 5′-TTACGCCAAGCTTGCATGCCTGCAGGTCGACTCTAGAGGATCCCCGTTTGCCTGGATACACGAAC (reverse). Cloned products were confirmed by sequence analysis. Human OSCP (hOSCP) cDNA (NM_001697) was purchased from GenScript and amplified using the following primers: 5′-CAGTGTGCTGGAATTCAACACAATGGCTGCCCCAGCAGTGTCC (forward) and 5′-GATATCTGCAGAATTTTAGACAATCTCCCGCATAGCCCTG (reverse). To substitute with the yeast putative mitochondrial import sequence at the N terminus of the OSCP gene (yhOSCP), we used the forward primer 5′-CAGTGTGCTGGAATTCAACACAATGTTTAATAGAGTCTTTACCAGGTCATTTGCATCAAGCTTAAGAGCTGCTGCTTCCAAAGCTGCTGCTCCCCCTCCTGTTCAGGTATACGGTATTG and the same reverse primer as for hOSCP. PCR products were cloned in pYES2-URA previously digested with EcoRI-HF using the In-Fusion HD cloning kit (Clontech), and resulting

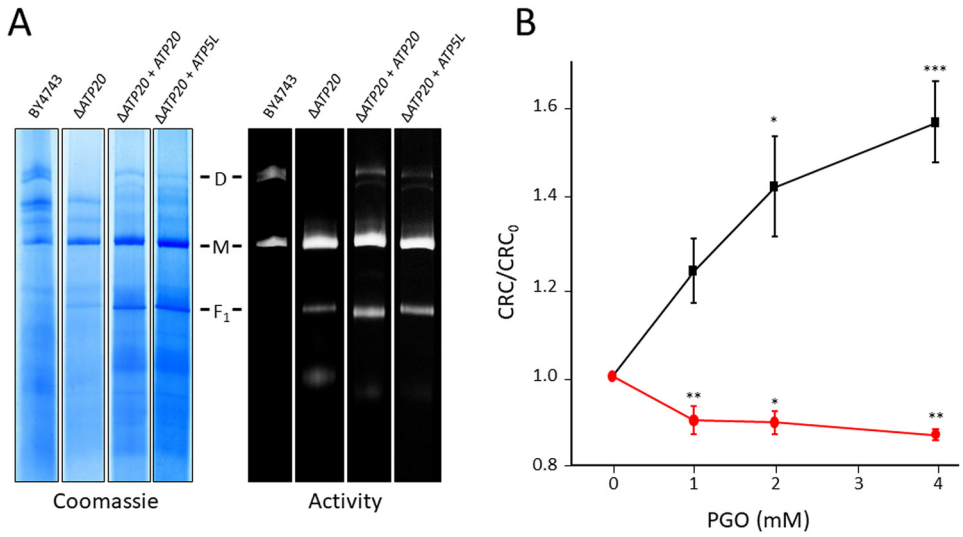

Figure 8. Expression of human subunit g in yeast prevents the inhibitory effect of PGO. *A*, yeast mitochondrial proteins of the indicated genotypes were separated by BN-PAGE as described under "Experimental Procedures" and revealed with Coomassie Blue and in-gel activity staining for ATP hydrolysis to identify dimers (*D*), monomers (*M*), and F_1 sector of F-ATP synthase. *B*, CRC of yeast mitochondria from Δ*ATP20* + *ATP20* (*black trace*) and Δ*ATP20* + *ATP5L* (*red trace*) pretreated with the indicated concentrations of PGO. Data are expressed as CRC/CRC_0 ratio, in which CRC_0 refers to the CRC of DMSO-treated mitochondria. Results are mean ± S.E. (*error bars*) of at least three independent experiments. *, $p < 0.05$ *versus* vehicle; **, $p < 0.01$ *versus* vehicle; ***, $p < 0.001$ *versus* vehicle. One-way ANOVA was used for statistical analysis.

vectors were checked by sequencing. Yeast Δ*ATP5* cells were separately transformed by a standard procedure (58) with yOSCP pFL38-URA, hOSCP pYES2-URA, or yhOSCP pYES2-URA, and correct clones were selected. Human cDNA *ATP5L* cloned into pESC-LEU vector by SalI/XhoI sites was purchased from GenScript. The oligonucleotide primers used for the yeast *ATP20* gene to be cloned in pESC-LEU vector by SalI/XhoI sites were 5′-GGGCCCGGGCGTCGACAACACAATGCTAAGC-AGGATCCAA (forward) and 5′-ACCAAGCTTACTCGATT-AGTGATGTTTATATCCCAC (reverse). PCR products were cloned in pESC-LEU vector previously digested with SalI-HF and XhoI using the In-Fusion HD cloning kit (Clontech), and resulting vectors were checked by sequencing. A one-step transformation protocol (58) was used to transform *ATP5L* pESC-LEU or ATP20 pESC-LEU into yeast Δ*ATP20* strain and cultured in the selective medium 2% galactose (drop-out leucine). The oligonucleotide primers used for TIM11 R8A and ATP20 R107A site-directed mutagenesis were as follows: TIM11 R8A, 5′-CGACAGTTAATGTTTTG**GC**ATACTCTG-CGTTGGGTTTG (forward) and 5′-CAAACCCAACGCAG-AGTAT**GC**CAAAACATTAACTGTCG (reverse); ATP20 R107A, 5′-CGGTGAAATAATTGGAAGA**GC**AAAATTAG-TGGGATATAAAC (forward) and 5′-GTTTATATCCCACT-AATTTT**GC**TCTTCCAATTATTTCACCG (reverse).

The QuikChange Lightning site-directed mutagenesis kit (Agilent) was used to harvest the mutants, and the dsDNA templates we used were *TIM11* and *ATP20* WT genes created in pFL38 plasmid. After the mutations were confirmed by sequencing, a one-step transformation protocol (58) was used to transform the plasmid into Δ*TIM11* or Δ*ATP20 S. cerevisiae* strain and plated on the selective medium 2% Glu (drop-out uracil) and incubated in 30 °C for 2 days.

Mouse liver mitochondria preparation

All of the isolation procedures were performed at 4 °C or on ice. Mouse livers were cut into pieces in the isolation buffer containing 250 mM sucrose, 10 mM Tris-HCl, 0.1 mM EGTA, pH 7.4. The homogenate suspension was centrifuged at 690 × *g* for 10 min. The supernatant was collected and centrifuged at 7000 × *g* for 10 min. The pellet was suspended in the isolation buffer and centrifuged at 9400 × *g* for 5 min. The mitochondria pellet was resuspended in about 400 μl of isolation buffer. The biuret test was used for determining protein concentration.

Yeast mitochondria isolation

Yeast mitochondria were isolated as described previously (19). Briefly, yeast cells were cultured in 400 ml of medium containing 1% yeast extract, 1% bacto-polypeptone, and 2% galactose overnight at 30 °C. Yeast cells were harvested by centrifugation at 2000 × *g* for 5 min at room temperature. The cell pellet was incubated in 0.1 M Tris-SO_4, pH 9.4, buffer, supplemented with 10 mM DTT for 15 min at 37 °C. The incubation was terminated by centrifugation at 2000 × *g* for 5 min and washed once with 1.2 M sorbitol, 20 mM P_i, pH 7.4, buffer. The cell pellet was resuspended in the above sorbitol buffer supplemented with zymolyase (0.4 mg/g pellet) and then incubated for 45 min at 30 °C. The incubation was terminated by centrifugation at 2000 × *g* for 5 min at 4 °C and washed once with sorbitol buffer. The cell pellet was resuspended in cold buffer containing 0.6 M mannitol, 10 mM Tris-HCl, 0.1 mM EDTA, pH 7.4, and homogenized with a Potter homogenizer. The supernatant was collected and centrifuged at 2000 × *g* for 5 min at 4 °C, and then the supernatant was centrifuged at 12,000 × *g* for 10 min at 4 °C. The mitochondrial pellet was harvested in mannitol medium. Protein concentration was quantified by the A_{280} of 0.6% SDS-solubilized mitochondria.

Cell permeabilization

The culture medium of human HEK293 cells was discarded, and cells were washed once with Dulbecco's PBS. Cells were

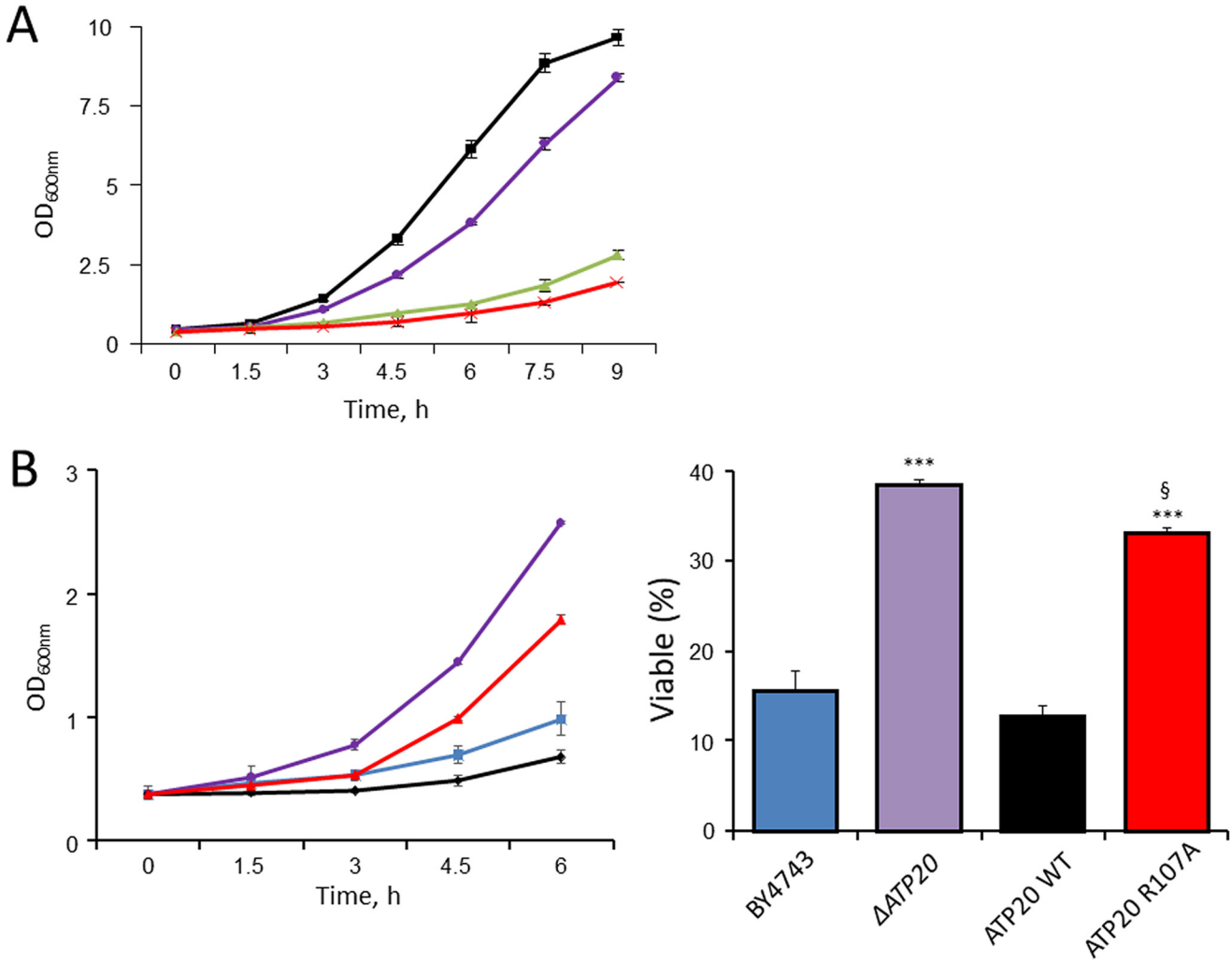

Figure 9. The ATP20 R107A yeast mutant is partially resistant to PGO toxicity. *A*, $A_{600\ nm}$ values of WT strain BY4743 cultured in 2% glucose (*black trace*), 20% glucose (*purple trace*), 2% glucose with the addition of 16 mM MGO (*green trace*), or 2% glucose with the addition of 0.5 mM PGO (*red trace*) at the indicated time points. *B* (*left*), $A_{600\ nm}$ value of yeast WT strain BY4743 (*blue trace*), Δ*ATP20* mutant (*purple trace*), ATP20 WT control (*black trace*), or ATP20 R107A (*red trace*) cultured in 2% glucose with the addition of 0.5 mM PGO. *Right*, survival of yeast cells incubated with 0.5 mM PGO at 30 °C for 6 h normalized to untreated cultures. Data are mean ± S.E. (*error bars*) of three independent experiments. ***, $p < 0.001$ *versus* BY4743; §, $p < 0.001$ *versus* ATP20 WT. One-way ANOVA was used for statistical analysis.

treated with 0.25% trypsin, and the reaction was terminated by the addition of culture medium. *Drosophila* S_2R^+ cells were detached with a scraper. Cell suspensions were centrifuged at 500 × *g* for 5 min and washed once with medium containing 130 mM KCl, 10 mM MOPS-Tris, 1 mM P_i, 0.1 mM EGTA, pH 7.4. The cell pellet was resuspended in a medium containing 130 mM KCl, 10 mM MOPS-Tris, 1 mM P_i, 1 mM EGTA, pH 7.4, and supplemented with 100 μM digitonin and incubated for 10 min on ice at a density of 2×10^7 cells/ml (HEK293 cells) or supplemented with 150 μM digitonin and incubated on ice for 20 min at a density of 6×10^7 cells/ml (*Drosophila* S_2R^+ cells). The incubations were terminated by dilution with 15–20 ml of medium containing 130 mM KCl, 10 mM MOPS-Tris, 1 mM P_i, 0.1 mM EGTA, pH 7.4, followed by centrifugation at 500 × *g* for 5 min at 4 °C. The cell pellet was washed once with 5 ml of the above KCl medium at 4 °C. The final pellet was resuspended in 250 mM sucrose, 20 μM EGTA, 10 mM HEPES-KOH, pH 8.0, for reaction with PGO.

Chemical modification with PGO

Freshly isolated mouse liver or yeast mitochondria (1 mg/ml) or 2×10^7/ml permeabilized cells were incubated with PGO in 250 mM sucrose, 20 μM EGTA, 10 mM HEPES-KOH, pH 8.0, for 15 min at 25 °C. The reaction was terminated by decreasing the pH to 6.8 with HEPES and cooling to 4 °C. Mitochondria were precipitated by centrifugation at 8000 × *g* for 6 min and washed once with 250 mM sucrose, 0.1 mM EGTA, 0.5 mg/ml BSA, 10 mM Tris-HCl, pH 7.4. Mitochondria or cells were finally resuspended in the assay medium.

Mitochondrial Ca^{2+} retention capacity

Yeast mitochondria (0.5 mg of protein/ml) were suspended in 250 mM sucrose, 10 mM Tris-MOPS, 20 μM EGTA, 1 mM NADH, 5 μM ETH129, 2 mM P_i, 1 μM Calcium Green-5N, 0.5 mg/ml BSA, pH 7.4. MLM (0.5 mg of protein/ml) and permeabilized HEK293 or *Drosophila* S_2R^+ cells (1×10^7 cells/ml) were suspended in 250 mM sucrose, 10 mM Tris-MOPS, 10 μM

EGTA, 1 mM P_i, 0.5 μM Calcium Green-5N, 5 mM succinate, 2 μM rotenone, pH 7.4. Final volume was 0.2 ml. External Ca^{2+} concentration was monitored by Calcium Green-5N fluorescence (excitation and emission wavelengths 485 and 538 nm, respectively) using a Fluoroskan Ascent FL (Thermo Scientific) plate reader.

Mitochondrial swelling assay

Isolated yeast mitochondria were suspended in 250 mM sucrose, 10 mM Tris-MOPS, 20 μM EGTA, 1 mM NADH, 5 μM ETH129, 0.5 mg/ml BSA, 2 mM P_i, pH 7.4, at a concentration of 0.5 mg of protein/ml in a final volume of 2 ml. Mitochondrial swelling was measured as the decrease of the turbidity (apparent absorbance at 540 nm) using a Cary 100 UV-visible spectrophotometer from Agilent Technologies.

Western blotting

Isolated mitochondria were lysed in 150 mM NaCl, 50 mM Tris-HCl, pH 7.4, 2 mM EDTA, 2 mM EGTA, 1% Triton X-100, 10 mM β-mercaptoethanol, 10% glycerol, 0.3% Nonidet P-40, 0.04% bromphenol blue, supplemented with protease inhibitor mixture (Sigma) at 2.5 μg of protein/μl and boiled for 5 min. The above lysates were loaded onto NuPAGE™ 12% BisTris protein gels (Invitrogen), and proteins were separated by electrophoresis in NuPAGE™ MOPS SDS running buffer (Invitrogen) for 3 h at 20 mA at 4 °C. Resolved proteins were transferred to nitrocellulose membranes in NuPAGE™ transfer buffer for 1.25 h at 30 V at 4 °C, followed by membrane blocking with 5% (w/v) dry milk. The membrane was incubated overnight with the antibodies for *TIM11*, *ATP20*, and γ subunits overnight at 4 °C. Immunoreactive bands were detected by chemiluminescence using an Uvitec Cambridge instrument.

Blue native gel electrophoresis

Isolated yeast mitochondria were suspended in 150 mM potassium acetate, 30 mM HEPES, 10% glycerol, 1 mM phenylmethylsulfonyl fluoride, supplemented with 1.5% (w/v) digitonin, pH 7.4, at 10 mg/ml, followed by centrifugation at 100,000 × *g* for 25 min at 4 °C with a Beckman TL-100 rotor. Supernatants were collected and supplemented with native PAGE 5% G-250 sample additive (Invitrogen) and then rapidly applied onto NativePAGE™ Novex™ 3–12% BisTris protein gels (Invitrogen). Electrophoresis was carried out in the Dark Blue cathode buffer at 150 V for 20 min and in the Light Blue cathode buffer at 250 V for 2 h. After electrophoresis, gels were stained with Coomassie Blue or used for in-gel activity staining of F-ATP synthase as described previously (19).

ATP hydrolysis assay

MLM or YM pretreated by PGO were suspended in 30 mM sucrose, 50 mM KCl, 50 mM Tris-HCl, 2 mM EGTA, 4 mM $MgCl_2$ and 2 mM phosphoenolpyruvate, supplemented with 4 units/ml pyruvate kinase, 3 units/ml lactate dehydrogenase, 2 mM ATP, and 0.3 mM NADH. Treatment with 4 μM oligomycin was performed at 37 °C for 15 min. The assay was carried out at 37 °C at a protein concentration of 40 μg × ml^{-1} in a final volume of 0.2 ml. ATP synthesis was measured as the decrease of absorbance of NADH at 340 nm using an Infinite® 200 PRO multimode microplate reader.

Oxygen consumption rate

A Clark oxygen electrode was used to detect the oxygen consumption rate of isolated mitochondria. MLM were incubated in 250 mM sucrose, 10 mM Tris-MOPS, 10 μM EGTA, pH 7.4, at a final concentration of 0.5 mg of protein/ml in a final volume of 2 ml. Further additions were 5 mM succinate as substrate, 1 mM P_i, and 0.2 mM ADP. YM were incubated in 250 mM sucrose, 10 mM Tris-MOPS, 20 μM EGTA, 5 mM P_i, 0.5 mg/ml BSA, pH 7.4, at a final concentration of 0.25 mg of protein/ml in a final volume of 2 ml. Further additions were 1 mM NADH, 0.2 mM ADP, and 4 μM oligomycin.

Mass spectrometry of g subunit peptides

Peptides (amino acids 88–114 of subunit g) modeled on the native sequence or containing alanine at position 106 were purchased from Caslo ApS (Kongens Lyngby, Denmark). Peptides were dissolved at a concentration of 100 μM in 10 mM Hepes-K^+, pH 8.0, and allowed to react with 2 mM PGO at room temperature for 60 min. The reaction was stopped by the addition of 0.5% TFA. The peptides were separated from the reaction mixture by reverse phase chromatography using C18 ZipTips (Millipore) pre-equilibrated with 0.5% TFA. Bound peptides were eluted with 10 μl of 60% acetonitrile and 0.5% TFA. The eluate was concentrated to 1 μl under a stream of nitrogen, mixed with 1 μl of a saturated solution of α-cyano-4-hydroxycinnamic acid, and applied to the MALDI target plate. MALDI-TOF was performed on a Bruker Ultraflextreme (Bremen, Germany) mass spectrometer operating in positive reflectron mode. Calibration of the instrument was performed using peptides of known mass.

Secondary structure assignment

This was performed pairing predictions from PSIPRED (59) and FELLS (60), whereas transmembrane regions were predicted with TMHMM (61). Default parameters were selected. The three-dimensional structure was visualized with Chimera (62).

Author contributions—L. G., M. C., and P. B. conceptualization; L. G. and P. B. data curation; L. G. and M. C. formal analysis; L. G., M. C., and O. E. investigation; L. G. and P. B. writing-original draft; M. C., G. S., V. P., and P. B. supervision; M. C. validation; M. C. and G. S. methodology; P. B. funding acquisition; P. B. writing-review and editing; G. M. bioinformatics analysis.

References

1. Hunter, D. R., Haworth, R. A., and Southard, J. H. (1976) Relationship between configuration, function, and permeability in calcium-treated mitochondria. *J. Biol. Chem.* **251,** 5069–5077 Medline
2. Kinnally, K. W., Campo, M. L., and Tedeschi, H. (1989) Mitochondrial channel activity studied by patch-clamping mitoplasts. *J. Bioenerg. Biomembr.* **21,** 497–506 CrossRef Medline
3. Petronilli, V., Szabò, I., and Zoratti, M. (1989) The inner mitochondrial membrane contains ion-conducting channels similar to those found in bacteria. *FEBS Lett.* **259,** 137–143 CrossRef Medline

4. Szabo, I., and Zoratti, M. (2014) Mitochondrial channels: ion fluxes and more. *Physiol. Rev.* **94,** 519–608 CrossRef Medline
5. Bernardi, P., and von Stockum, S. (2012) The permeability transition pore as a Ca^{2+} release channel: new answers to an old question. *Cell Calcium* **52,** 22–27 CrossRef Medline
6. Petronilli, V., Penzo, D., Scorrano, L., Bernardi, P., and Di Lisa, F. (2001) The mitochondrial permeability transition, release of cytochrome *c* and cell death: correlation with the duration of pore openings *in situ*. *J. Biol. Chem.* **276,** 12030–12034 CrossRef Medline
7. Giorgio, V., Guo, L., Bassot, C., Petronilli, V., and Bernardi, P. (2018) Calcium and regulation of the mitochondrial permeability transition. *Cell Calcium* **70,** 56–63 CrossRef Medline
8. Bernardi, P., Rasola, A., Forte, M., and Lippe, G. (2015) The mitochondrial permeability transition pore: channel formation by F-ATP synthase, integration in signal transduction, and role in pathophysiology. *Physiol. Rev.* **95,** 1111–1155 CrossRef Medline
9. Nicolli, A., Petronilli, V., and Bernardi, P. (1993) Modulation of the mitochondrial cyclosporin A-sensitive permeability transition pore by matrix pH: evidence that the pore open-closed probability is regulated by reversible histidine protonation. *Biochemistry* **32,** 4461–4465 CrossRef Medline
10. Petronilli, V., Costantini, P., Scorrano, L., Colonna, R., Passamonti, S., and Bernardi, P. (1994) The voltage sensor of the mitochondrial permeability transition pore is tuned by the oxidation-reduction state of vicinal thiols: increase of the gating potential by oxidants and its reversal by reducing agents. *J. Biol. Chem.* **269,** 16638–16642 Medline
11. Costantini, P., Chernyak, B. V., Petronilli, V., and Bernardi, P. (1996) Modulation of the mitochondrial permeability transition pore by pyridine nucleotides and dithiol oxidation at two separate sites. *J. Biol. Chem.* **271,** 6746–6751 CrossRef Medline
12. Eriksson, O., Fontaine, E., and Bernardi, P. (1998) Chemical modification of arginines by 2,3-butanedione and phenylglyoxal causes closure of the mitochondrial permeability transition pore. *J. Biol. Chem.* **273,** 12669–12674 CrossRef Medline
13. Linder, M. D., Morkunaite-Haimi, S., Kinnunen, P. K. J., Bernardi, P., and Eriksson, O. (2002) Ligand-selective modulation of the permeability transition pore by arginine modification: opposing effects of *p*-hydroxyphenylglyoxal and phenylglyoxal. *J. Biol. Chem.* **277,** 937–942 CrossRef Medline
14. Speer, O., Morkunaite-Haimi, S., Liobikas, J., Franck, M., Hensbo, L., Linder, M. D., Kinnunen, P. K. J., Wallimann, T., and Eriksson, O. (2003) Rapid suppression of mitochondrial permeability transition by methylglyoxal: role of reversible arginine modification. *J. Biol. Chem.* **278,** 34757–34763 CrossRef Medline
15. Johans, M., Milanesi, E., Franck, M., Johans, C., Liobikas, J., Panagiotaki, M., Greci, L., Principato, G., Kinnunen, P. K. J., Bernardi, P., Costantini, P., and Eriksson, O. (2005) Modification of permeability transition pore arginine(s) by phenylglyoxal derivatives in isolated mitochondria and mammalian cells: structure-function relationship of arginine ligands. *J. Biol. Chem.* **280,** 12130–12136 CrossRef Medline
16. Bonora, M., Bononi, A., De Marchi, E., Giorgi, C., Lebiedzinska, M., Marchi, S., Patergnani, S., Rimessi, A., Suski, J. M., Wojtala, A., Wieckowski, M. R., Kroemer, G., Galluzzi, L., and Pinton, P. (2013) Role of the c subunit of the F_O ATP synthase in mitochondrial permeability transition. *Cell Cycle* **12,** 674–683 CrossRef Medline
17. Giorgio, V., von Stockum, S., Antoniel, M., Fabbro, A., Fogolari, F., Forte, M., Glick, G. D., Petronilli, V., Zoratti, M., Szabó, I., Lippe, G., and Bernardi, P. (2013) Dimers of mitochondrial ATP synthase form the permeability transition pore. *Proc. Natl. Acad. Sci. U.S.A.* **110,** 5887–5892 CrossRef Medline
18. Alavian, K. N., Beutner, G., Lazrove, E., Sacchetti, S., Park, H. A., Licznerski, P., Li, H., Nabili, P., Hockensmith, K., Graham, M., Porter, G. A., Jr., and Jonas, E. A. (2014) An uncoupling channel within the c-subunit ring of the F_1F_O ATP synthase is the mitochondrial permeability transition pore. *Proc. Natl. Acad. Sci. U.S.A.* **111,** 10580–10585 CrossRef Medline
19. Carraro, M., Giorgio, V., Šileikyte, Sartori, G., Forte, M., Lippe, G., Zoratti, M., Szabò, I., and Bernardi, P. (2014) Channel formation by yeast F-ATP synthase and the role of dimerization in the mitochondrial permeability transition. *J. Biol. Chem.* **289,** 15980–15985 CrossRef Medline
20. von Stockum, S., Giorgio, V., Trevisan, E., Lippe, G., Glick, G. D., Forte, M. A., Da-Rè, C., Checchetto, V., Mazzotta, G., Costa, R., Szabò, I., and Bernardi, P. (2015) F-ATPase of *D. melanogaster* forms 53 picosiemen (53-pS) channels responsible for mitochondrial Ca^{2+}-induced Ca^{2+} release. *J. Biol. Chem.* **290,** 4537–4544 CrossRef Medline
21. Giorgio, V., Burchell, V., Schiavone, M., Bassot, C., Minervini, G., Petronilli, V., Argenton, F., Forte, M., Tosatto, S., Lippe, G., and Bernardi, P. (2017) Ca^{2+} binding to F-ATP synthase β subunit triggers the mitochondrial permeability transition. *EMBO Rep.* **18,** 1065–1076 CrossRef Medline
22. Antoniel, M., Jones, K., Antonucci, S., Spolaore, B., Fogolari, F., Petronilli, V., Giorgio, V., Carraro, M., Di Lisa, F., Forte, M., Szabó, I., Lippe, G., and Bernardi, P. (2018) The unique histidine in OSCP subunit of F-ATP synthase mediates inhibition of the permeability transition pore by acidic pH. *EMBO Rep.* **19,** 257–268 CrossRef Medline
23. He, J., Ford, H. C., Carroll, J., Ding, S., Fearnley, I. M., and Walker, J. E. (2017) Persistence of the mitochondrial permeability transition in the absence of subunit c of human ATP synthase. *Proc. Natl. Acad. Sci. U.S.A.* **114,** 3409–3414 CrossRef Medline
24. He, J., Carroll, J., Ding, S., Fearnley, I. M., and Walker, J. E. (2017) Permeability transition in human mitochondria persists in the absence of peripheral stalk subunits of ATP synthase. *Proc. Natl. Acad. Sci. U.S.A.* **114,** 9086–9091 CrossRef Medline
25. Bernardi, P., and Lippe, G. (2018) Channel formation by F-ATP synthase and the permeability transition pore: an update. *Curr. Opin. Physiol.* **3,** 1–5 CrossRef
26. Oya, T., Hattori, N., Mizuno, Y., Miyata, S., Maeda, S., Osawa, T., and Uchida, K. (1999) Methylglyoxal modification of protein: chemical and immunochemical characterization of methylglyoxal-arginine adducts. *J. Biol. Chem.* **274,** 18492–18502 CrossRef Medline
27. Ellis, E. M. (2007) Reactive carbonyls and oxidative stress: potential for therapeutic intervention. *Pharmacol. Ther.* **115,** 13–24 CrossRef Medline
28. Maessen, D. E., Stehouwer, C. D., and Schalkwijk, C. G. (2015) The role of methylglyoxal and the glyoxalase system in diabetes and other age-related diseases. *Clin. Sci.* **128,** 839–861 CrossRef Medline
29. Martins, A. M., Cordeiro, C. A., and Ponces Freire, A. M. (2001) *In situ* analysis of methylglyoxal metabolism in *Saccharomyces cerevisiae*. *FEBS Lett.* **499,** 41–44 CrossRef Medline
30. Gomes, R. A., Sousa Silva, M., Vicente Miranda, H., Ferreira, A. E., Cordeiro, C. A., and Freire, A. P. (2005) Protein glycation in *Saccharomyces cerevisiae*: argpyrimidine formation and methylglyoxal catabolism. *FEBS J.* **272,** 4521–4531 CrossRef Medline
31. Gomes, R. A., Vicente Miranda, H., Sousa Silva, M., Graça, G., Coelho, A. V., do Nascimento Ferreira, A. E., Cordeiro, C., and Freire, A. P. (2008) Protein glycation and methylglyoxal metabolism in yeast: finding peptide needles in protein haystacks. *FEMS Yeast Res.* **8,** 174–181 CrossRef Medline
32. Baker, L. A., Watt, I. N., Runswick, M. J., Walker, J. E., and Rubinstein, J. L. (2012) Arrangement of subunits in intact mammalian mitochondrial ATP synthase determined by cryo-EM. *Proc. Natl. Acad. Sci. U.S.A.* **109,** 11675–11680 CrossRef Medline
33. Davies, K. M., Anselmi, C., Wittig, I., Faraldo-Gómez, J. D., and Kühlbrandt, W. (2012) Structure of the yeast F_1F_o-ATP synthase dimer and its role in shaping the mitochondrial cristae. *Proc. Natl. Acad. Sci. U.S.A.* **109,** 13602–13607 CrossRef Medline
34. Allegretti, M., Klusch, N., Mills, D. J., Vonck, J., Kühlbrandt, W., and Davies, K. M. (2015) Horizontal membrane-intrinsic α-helices in the stator a-subunit of an F-type ATP synthase. *Nature* **521,** 237–240 CrossRef Medline
35. Hahn, A., Parey, K., Bublitz, M., Mills, D. J., Zickermann, V., Vonck, J., Kühlbrandt, W., and Meier, T. (2016) Structure of a complete ATP synthase dimer reveals the molecular basis of inner mitochondrial membrane morphology. *Mol. Cell* **63,** 445–456 CrossRef Medline
36. Guo, H., Bueler, S. A., and Rubinstein, J. L. (2017) Atomic model for the dimeric F_O region of mitochondrial ATP synthase. *Science* **358,** 936–940 CrossRef Medline
37. He, J., Ford, H. C., Carroll, J., Douglas, C., Gonzales, E., Ding, S., Fearnley, I. M., and Walker, J. E. (2018) Assembly of the membrane domain of ATP

synthase in human mitochondria. *Proc. Natl. Acad. Sci. U.S.A.* **115,** 2988–2993 CrossRef Medline
38. Zeng, J., and Davies, M. J. (2005) Evidence for the formation of adducts and *S*-(carboxymethyl)cysteine on reaction of α-dicarbonyl compounds with thiol groups on amino acids, peptides, and proteins. *Chem. Res. Toxicol.* **18,** 1232–1241 CrossRef Medline
39. Mitome, N., Ono, S., Sato, H., Suzuki, T., Sone, N., and Yoshida, M. (2010) Essential arginine residue of the F_o: a subunit in F_oF_1-ATP synthase has a role to prevent the proton shortcut without c-ring rotation in the F_o proton channel. *Biochem. J.* **430,** 171–177 CrossRef Medline
40. Uh, M., Jones, D., and Mueller, D. M. (1990) The gene coding for the yeast oligomycin sensitivity-conferring protein. *J. Biol. Chem.* **265,** 19047–19052 Medline
41. Prescott, M., Bush, N. C., Nagley, P., and Devenish, R. J. (1994) Properties of yeast cells depleted of the OSCP subunit of mitochondrial ATP synthase by regulated expression of the ATP5 gene. *Biochem. Mol. Biol. Int.* **34,** 789–799 Medline
42. Lee, C. F., Chavez, J. D., Garcia-Menendez, L., Choi, Y., Roe, N. D., Chiao, Y. A., Edgar, J. S., Goo, Y. A., Goodlett, D. R., Bruce, J. E., and Tian, R. (2016) Normalization of NAD^+ redox balance as a therapy for heart failure. *Circulation* **134,** 883–894 CrossRef Medline
43. Burstein, S. R., Kim, H. J., Fels, J. A., Qian, L., Zhang, S., Zhou, P., Starkov, A. A., Iadecola, C., and Manfredi, G. (2018) Estrogen receptor β modulates permeability transition in brain mitochondria. *Biochim. Biophys. Acta* **1859,** 423–433 CrossRef Medline
44. Allen, R. D. (1995) Membrane tubulation and proton pumps. *Protoplasma* **189,** 1–8 CrossRef
45. Dudkina, N. V., Sunderhaus, S., Braun, H. P., and Boekema, E. J. (2006) Characterization of dimeric ATP synthase and cristae membrane ultrastructure from *Saccharomyces* and *Polytomella* mitochondria. *FEBS Lett.* **580,** 3427–3432 CrossRef Medline
46. Paumard, P., Vaillier, J., Coulary, B., Schaeffer, J., Soubannier, V., Mueller, D. M., Brèthes, D., di Rago, J. P., and Velours, J. (2002) The ATP synthase is involved in generating mitochondrial cristae morphology. *EMBO J.* **21,** 221–230 CrossRef Medline
47. Arnold, I., Pfeiffer, K., Neupert, W., Stuart, R. A., and Schägger, H. (1998) Yeast mitochondrial F_1F_0-ATP synthase exists as a dimer: identification of three dimer-specific subunits. *EMBO J.* **17,** 7170–7178 CrossRef Medline
48. Arselin, G., Giraud, M. F., Dautant, A., Vaillier, J., Brèthes, D., Coulary-Salin, B., Schaeffer, J., and Velours, J. (2003) The GxxxG motif of the transmembrane domain of subunit e is involved in the dimerization/oligomerization of the yeast ATP synthase complex in the mitochondrial membrane. *Eur. J. Biochem.* **270,** 1875–1884 CrossRef Medline
49. Arselin, G., Vaillier, J., Salin, B., Schaeffer, J., Giraud, M. F., Dautant, A., Brèthes, D., and Velours, J. (2004) The modulation in subunits e and g amounts of yeast ATP synthase modifies mitochondrial cristae morphology. *J. Biol. Chem.* **279,** 40392–40399 CrossRef Medline
50. Strauss, M., Hofhaus, G., Schröder, R. R., and Kühlbrandt, W. (2008) Dimer ribbons of ATP synthase shape the inner mitochondrial membrane. *EMBO J.* **27,** 1154–1160 CrossRef Medline
51. Wittig, I., Velours, J., Stuart, R., and Schägger, H. (2008) Characterization of domain interfaces in monomeric and dimeric ATP synthase. *Mol. Cell. Proteomics* **7,** 995–1004 CrossRef Medline
52. Habersetzer, J., Ziani, W., Larrieu, I., Stines-Chaumeil, C., Giraud, M. F., Brèthes, D., Dautant, A., and Paumard, P. (2013) ATP synthase oligomerization: from the enzyme models to the mitochondrial morphology. *Int. J. Biochem. Cell Biol.* **45,** 99–105 CrossRef Medline
53. Madeo, F., Fröhlich, E., Ligr, M., Grey, M., Sigrist, S. J., Wolf, D. H., and Fröhlich, K. U. (1999) Oxygen stress: a regulator of apoptosis in yeast. *J. Cell Biol.* **145,** 757–767 CrossRef Medline
54. Carraro, M., and Bernardi, P. (2016) Calcium and reactive oxygen species in regulation of the mitochondrial permeability transition and of programmed cell death in yeast. *Cell Calcium* **60,** 102–107 CrossRef Medline
55. Laun, P., Büttner, S., Rinnerthaler, M., Burhans, W. C., and Breitenbach, M. (2012) Yeast aging and apoptosis. *Subcell. Biochem.* **57,** 207–232 Medline
56. Lindblom, R., Higgins, G., Coughlan, M., and de Haan, J. B. (2015) Targeting mitochondria and reactive oxygen species-driven pathogenesis in diabetic nephropathy. *Rev. Diabet. Stud.* **12,** 134–156 CrossRef Medline
57. von Stockum, S., Basso, E., Petronilli, V., Sabatelli, P., Forte, M. A., and Bernardi, P. (2011) Properties of Ca^{2+} transport in mitochondria of *Drosophila melanogaster*. *J. Biol. Chem.* **286,** 41163–41170 CrossRef Medline
58. Chen, D. C., Yang, B. C., and Kuo, T. T. (1992) One-step transformation of yeast in stationary phase. *Curr. Genet.* **21,** 83–84 CrossRef Medline
59. Buchan, D. W., Minneci, F., Nugent, T. C., Bryson, K., and Jones, D. T. (2013) Scalable web services for the PSIPRED Protein Analysis Workbench. *Nucleic Acids Res.* **41,** W349–W357 CrossRef Medline
60. Piovesan, D., Walsh, I., Minervini, G., and Tosatto, S. C. E. (2017) FELLS: fast estimator of latent local structure. *Bioinformatics* **33,** 1889–1891 CrossRef Medline
61. Krogh, A., Larsson, B., von Heijne, G., and Sonnhammer, E. L. (2001) Predicting transmembrane protein topology with a hidden Markov model: application to complete genomes. *J. Mol. Biol.* **305,** 567–580 CrossRef Medline
62. Pettersen, E. F., Goddard, T. D., Huang, C. C., Couch, G. S., Greenblatt, D. M., Meng, E. C., and Ferrin, T. E. (2004) UCSF Chimera: a visualization system for exploratory research and analysis. *J. Comput. Chem.* **25,** 1605–1612 CrossRef Medline
63. Petronilli, V., Cola, C., Massari, S., Colonna, R., and Bernardi, P. (1993) Physiological effectors modify voltage sensing by the cyclosporin A-sensitive permeability transition pore of mitochondria. *J. Biol. Chem.* **268,** 21939–21945 Medline

Arginine 107 of yeast ATP synthase subunit g mediates sensitivity of the mitochondrial permeability transition to phenylglyoxal

Lishu Guo, Michela Carraro, Geppo Sartori, Giovanni Minervini, Ove Eriksson, Valeria Petronilli and Paolo Bernardi

J. Biol. Chem. 2018, 293:14632-14645.
doi: 10.1074/jbc.RA118.004495 originally published online August 9, 2018